European Journal of Nuclear Medicine and Molecular Imaging (2019) 46:376–384
https://doi.org/10.1007/s00259-018-4183-0

ORIGINAL ARTICLE

Myocardial MIBG scintigraphy in genetic Parkinson's disease as a model for Lewy body disorders

Iñigo Gabilondo[1,2] · Verónica Llorens[1,3] · Trinidad Rodriguez[3] · Manuel Fernández[1,2,4] · Tomas Pérez Concha[2] · Marian Acera[1] · Beatriz Tijero[1,2] · Ane Murueta-Goyena[1] · Rocío del Pino[1] · Jesús Cortés[5,6,7] · Juan Carlos Gómez-Esteban[1,2,4]

Received: 5 July 2018 / Accepted: 17 September 2018 / Published online: 15 October 2018

Abstract

Purpose To identify myocardial sympathetic denervation patterns suggestive of Lewy body (LB) pathology in patients with genetic and idiopathic parkinsonisms by ^{123}I-metaiodobenzylguanidine (MIBG) scintigraphy.

Methods We retrospectively analysed myocardial MIBG images acquired with a dual-head gamma camera and low-energy high-resolution collimator (LEHR) in 194 patients with suspected synucleinopathy or atypical parkinsonism, including 34 with genetic Parkinson's disease (PD; 4 PARK1, 8 PARK2 and 22 PARK8), 85 with idiopathic PD (iPD), 6 with idiopathic REM sleep behaviour disorder (iRBD), 17 with dementia with LB (DLB), 40 with multiple system atrophy (MSA) and 12 with progressive supranuclear palsy (PSP), and in 45 healthy controls. We calculated heart-to-mediastinum MIBG uptake ratios (HMR) at 15 min and 4 h (HMR4H) for the LEHR and standardized medium-energy collimators, to obtain classification accuracies and optimal cut-off values for HMR using supervised classification and ROC analyses.

Results While patients with LB disorders had markedly lower $HMR4H_{LEHR}$ than controls (controls 1.86 ± 0.26, iPD 1.38 ± 0.29, iRBD 1.23 ± 0.09, PARK1 1.20 ± 0.09, DLB 1.17 ± 0.11; $p < 0.05$), for the remaining patient categories differences were smaller (PARK8 1.51 ± 0.32; $p < 0.05$) or not significant (MSA 1.82 ± 0.37, PSP 1.59 ± 0.23, PARK2 1.51 ± 0.30; $p > 0.05$). The diagnostic accuracy of $HMR4H_{LEHR}$ was highest in patients with LB disorders (PARK1, iPD, DLB, iRBD; 89% to 97%) and lowest in those with PARK2, PARK8, PSP and MSA (65% to 76%), with an optimal $HMR4H_{LEHR}$ cut-off value of 1.72 for discriminating most patients with LB disorders including iPD and 1.40 for discriminating those with aggressive LB spectrum phenotypes (DLB, PARK1 and iRBD).

Conclusion Our study including patients with a wide spectrum of genetic and idiopathic parkinsonisms with different degrees of LB pathology further supports myocardial MIBG scintigraphy as an accurate tool for discriminating patients with LB spectrum disorders.

Keywords Parkinson's disease · MIBG cardiac scintigraphy · Dysautonomia · Genetic · Alpha-synuclein

Electronic supplementary material The online version of this article (https://doi.org/10.1007/s00259-018-4183-0) contains supplementary material, which is available to authorized users.

✉ Iñigo Gabilondo
igabilon@gmail.com

[1] Neurodegenerative Diseases Group, Biocruces-Bizkaia Health Research Institute, Plaza de Cruces 12, CP 48903 Barakaldo, Bizkaia, Spain

[2] Neurology Department, Cruces University Hospital, Barakaldo, Bizkaia, Spain

[3] Nuclear Medicine Department, Cruces University Hospital, Barakaldo, Bizkaia, Spain

[4] Department of Neurosciences, University of the Basque Country (UPV/EHU), Leioa, Spain

[5] Computational Neuroimaging Group, Biocruces-Bizkaia Health Research Institute, Barakaldo, Bizkaia, Spain

[6] Ikerbasque: The Basque Foundation for Science, Bilbao, Spain

[7] Department of Cell Biology and Histology, University of the Basque Country (UPV/EHU), Leioa, Spain

Introduction

Metaiodobenzylguanidine (MIBG) is a physiological analogue of noradrenaline, which is actively transported to and stored in granules in presynaptic sympathetic nerve endings. Myocardial ^{123}I-MIBG uptake correlates with the integrity of postganglionic sympathetic cardiac nerves and thus ^{123}I-MIBG scintigraphy is able to quantify noninvasively the extent of myocardial denervation in patients with synucleinopathies and atypical parkinsonisms, helping with the differential diagnosis [1]. Several myocardial ^{123}I-MIBG scintigraphy studies have consistently demonstrated decreased myocardial noradrenergic innervation in patients with idiopathic Parkinson's disease (iPD) [2], pure autonomic failure, idiopathic REM sleep behaviour disorder (iRBD) [3] and dementia with Lewy bodies (DLB). In contrast, in a high proportion of patients with atypical parkinsonism, such as multiple system atrophy (MSA) and progressive supranuclear palsy (PSP), the results of myocardial scintigraphy are normal [4]. Interestingly, patients with the highest risk of developing a diffuse and severe Lewy body (LB) pathology in the CNS are those with highest degree of myocardial denervation on MIBG imaging [5–8].

Various genetic variants of PD constitute clinically and neuropathologically homogeneus groups of patients, including those with aggressive LB pathology such as carriers of the alpha-synuclein (SNCA) gene mutation (PARK1) [9], patients with variable degrees of LB disease such as carriers of the Leucine-Rich Repeat Kinase 2 (LRRK2) gene mutation (PARK8) and patients virtually free of LB pathology such as carriers of the Parkin gene mutation (PARK2). The use of myocardial MIBG scintigraphy in such genetic groups may provide additional evidence to validate the diagnostic performance of MIBG scintigraphy as an early biomarker of LB spectrum disorders [10–13].

The aim of the present study was to evaluate the degree of myocardial sympathetic denervation as measured by MIBG scintigraphy in patients with a wide spectrum of genetic and idiopathic parkinsonisms and related disorders, with special interest in comparing MIBG denervation trends in patients with severe LB pathology phenotypes (PARK1 carriers, DLB and iRBD) and those with less or absent LBs (PARK2 carriers, MSA, PSP and controls). We also aimed to identify the optimal cut-off values for myocardial MIBG metrics and their respective accuracies in discriminating healthy individuals from parkinsonism patients.

Materials and methods

Study design and selection of participants

We retrospectively analysed patients with suspected synucleinopathy or atypical parkinsonism who had undergone myocardial MIBG scintigraphy for clinical reasons in the Movement Disorders Unit and the Nuclear Medicine Department of Cruces University Hospital during the period 2007 to 2017. We identified a total of 194 patients: 34 with genetic PD who were all symptomatic mutation carriers, including E46K-SNCA (PARK1, $n = 4$), PARK2 ($n = 8$) and PARK8 ($n = 22$), 85 with iPD, 6 with iRBD (probable or confirmed by polysomnography), 17 with DLB, 40 with probable MSA, and 12 with probable PSP. We did not include patients with levodopa-resistant iPD because of their pathophysiological peculiarities as compared with classic levodopa-responsive iPD [14]. We also selected 45 healthy controls (HC) who had undergone MIBG scintigraphy as routine screening for suspicion of neurovascular dysautonomia. We reviewed all electronic clinical records to gather basic demographic data and disease-related information. We also identified a set of factors different from LB pathology influencing the structural or functional integrity of myocardial innervation, excluding all subjects with known heart failure (or other structural heart disease) and microvascular diabetic complications.

To further rule out heart failure, segmental myocardial function or perfusion defects, in addition to MIBG scintigraphy, all subjects underwent ECG-gated myocardial ^{99m}Tc-6-methoxy isobutyl isonitrile (^{99m}Tc-6-MIBI) single-photon emission computed tomography (SPECT) under resting conditions. Two nuclear medicine specialists (V.L. and T.R.) analysed the ECG-gated ^{99m}Tc-6-MIBI SPECT images to identify and quantify abnormalities in global and regional myocardial perfusion, to determine the left ventricular ejection fraction and total diastolic and systolic volumes, and to identify abnormalities in ventricular wall movement and thickness. For simplicity, we excluded all subjects in whom analysis of resting ^{99m}Tc-6-MIBI images revealed impaired left ventricle function (ejection fraction below 50%), severe regional myocardial hypoperfusion and/or ventricular wall movement or thickness abnormalities consistent in distribution with any known coronary territory, if it was not contradicted by subsequent cardiological evaluations, assuring myocardial structural and functional integrity. Lastly, 7 days before MIBG imaging, all subjects were asked to discontinue any sympathicomimetics, antihypertensive drugs, tricyclic antidepressants and antipsychotics known to affect MIBG uptake, unless strictly necessary for medical reasons [15]. All participants provided signed specific written informed consent for myocardial imaging and for the codified recording of their clinical and imaging data in the registry of our Movement Disorders Unit. The protocol for this study was approved by the local ethics committee.

Myocardial image acquisition and analysis

Myocardial ^{123}I-MIBG scintigraphy and ECG-gated ^{99m}Tc-6-MIBI SPECT images were acquired with a dual-head gamma camera system (Infinia; GE Healthcare, Milwaukee, WI,

USA) equipped with a low-energy high-resolution (LEHR) parallel-hole collimator. The acquisition and analysis of myocardial MIBG images were performed according to standard guidelines [16]. A detailed description of the protocols for both MIBG scintigraphy and ECG-gated ^{99m}Tc-6-MIBI SPECT can be found in the Supplementary material that includes MIBG imaging in example patients. For MIBG image quantification, two nuclear medicine specialists (V.L. and T.R.) manually drew three regions of interest (ROIs) in the heart, lung and upper mediastinum (avoiding the thyroid gland; Supplementary Fig. 1). To increase the accuracy of ROI positioning and to avert potential segmentation errors on MIBG images due to low tracer uptake in the heart, the silhouettes of the myocardium were first delineated using anterior MIBI images (anatomical reference). The mean count density for each ROI was obtained and the heart-to-mediastinum ratios (HMR) were calculated for MIBG uptake in the early phase (15 min) and delayed phase (4 h; HMR15M and HMR4H, respectively).

To obtain a measure of the balance between intraneuronal and extraneuronal binding and clearance of myocardial MIBG (sympathetic neuronal activity and integrity in the heart), the myocardial MIBG wash-out percentage was calculated using the formula: $[(HMR15M_{LEHR} - HMR4H_{LEHR})/HMR15M_{LEHR}] \times 100$. Instead of subtracting background (mediastinum) counts from heart counts as used in previous studies [8], in the present work we used the MIBG uptake HMR to calculate early to late myocardial MIBG wash-out. To improve the generalizability of our results, the HMR values are presented both as raw LEHR HMR values obtained with the LEHR collimator ($HMR15M_{LEHR}$ and $HMR4H_{LEHR}$) and as standardized HMR values for ME collimators ($HMR15M_{STD}$ and $HMR4H_{STD}$) calculated using the formula and conversion factor for LEHR (0.553) provided in the cross-calibration phantom study by Verschure et al. [17]. This was performed because calculated HMR values vary among institutions and studies depending on the characteristics of the collimator used: HMR values are higher if a medium-energy (ME) collimator is used than if a low-energy (LE) collimator is used [18]. Furthermore, the use of ME collimators is recommended in myocardial ^{123}I-MIBG imaging and are widely used in this application [16]. Further information on myocardial image acquisition and analysis is provided in the Supplementary material.

Data analysis, classification accuracy and optimal MIBG cut-off values

We first calculated proportions, means and standard deviations and assessed differences between diagnostic categories using the Kruskal-Wallis ANOVA for continuous variables (age, disease duration and MIBG metrics) and the pairwise Fisher's exact test for categorical variables (gender and presence of diabetes) using SPSS Statistics for Windows version 20.0 (IBM Corp., Armonk, NY, USA). We ranked diagnostic categories according to their respective median HMR4H values following the Jonckheere-Terpstra nonparametric rank test (see Fig. 1) and grouped them into clusters to test the diagnostic performance of HMR in nine different classification schemes (S1 to S9). We calculated the optimal cut-off values for HMR4H ($HMR4H_{LEHR}$ and $HMR4H_{STD}$) and HMR15M ($HMR15M_{LEHR}$ and $HMR15M_{STD}$) in each classification scheme (S1 to S9) using two approaches: (1) maximization of discrimination accuracy with the supervised classification algorithm "classification and regression tree" (CART); and (2) maximization of discrimination sensitivity and specificity with nonparametric receiver operating characteristic (ROC) analyses. Since the aim of each approach was to maximize different classification parameters, discrepancies in cut-off values were expected [19]. We implemented CART in the Waikato Environment for Knowledge Analysis (WEKA) [20] obtaining for each classification strategy baseline accuracy (proportion of patients with respect to the total number of subjects within each strategy), CART training accuracy and CART K-fold ($K = 10$) cross-validation accuracy. ROC analyses were implemented under SPSS, obtaining for each classification scheme ROC curves, areas under the curve (AUC) and the optimal cut-off values with respective sensitivities and specificities by maximizing the value of Youden's index [21]. Further descriptions of the methodology used for data analysis is provided in the Supplementary material.

Results

As the first main result of our study, there was a clear-cut spectrum of progressive myocardial MIBG uptake deficit, both for HMR15M and HMR4H, that was related to the severity of LB pathology attributed to each diagnostic category, with the highest average HMR values found in HC and patients with MSA and PSP, and the lowest values in patients with iPD, iRBD and DLB (Table 1, Fig. 1 and Supplementary Fig. 1). There were no statistically significant differences in HMR values between patients with genetic PD variants known to have mild or absent LB pathology (PARK2) and patients with MSA or HC. Similarly, we did not find significant differences ($p > 0.05$) in HMR values between genetic carriers with severe LB disease (PARK1) and patients with iRBD or DLB.

As the second main finding of our study, CART and ROC analyses demonstrated that HMR4H (but not HMR15M) provided excellent performance in discriminating between HC and patients with moderate to severe LB pathology (Table 2 and Fig. 2). Moreover, the classification algorithms showed that the best $HMR4H_{LEHR}$ cut-off value for discriminating most patients with LB spectrum disorders including those with iPD was 1.72 ($HMR4H_{STD}$ 2.15) and that the best

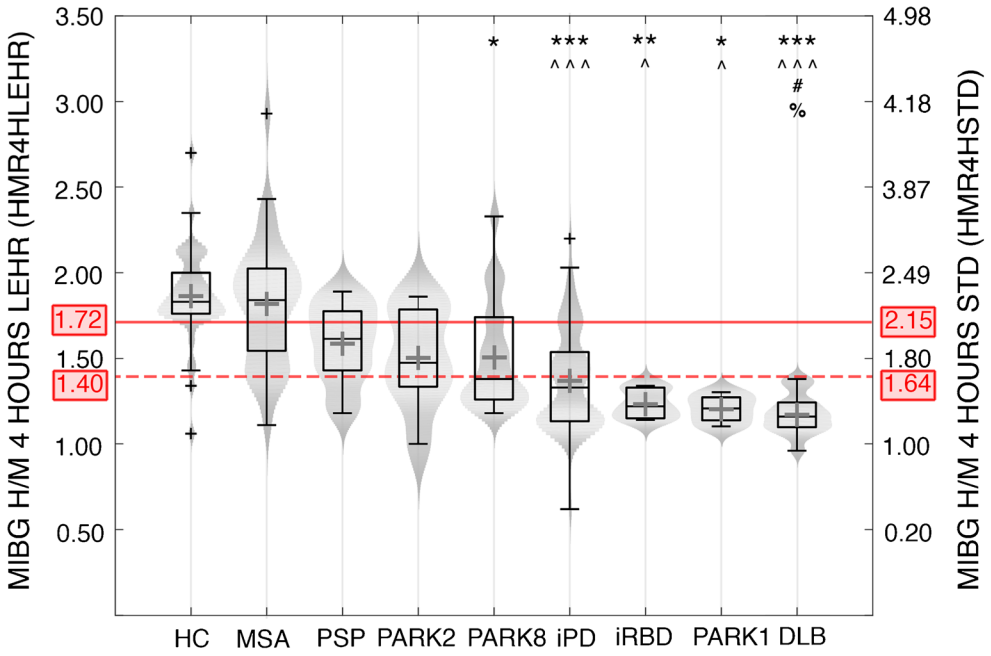

Fig. 1 Boxplots and violin plots for delayed myocardial MIBG uptake ratios (HMR4H) from anterior scintigraphy images in all diagnostic groups. Within each violin, both the grey level of the background and the horizontal distance between left and right curved boundaries at every HMR4H value represent the probability density of the HMR4H distribution of each diagnostic group. Abbreviations: *MIBG* ^{131}I- metaiodobenzylguanidine, *MIBG H/M 4 HOURS* heart-tomediastinum ratio for myocardial MIBG uptake after 4 h, *LEHR* low-energy high-resolution, *STD* standard, *HMR4HLEHR* HMR4H values obtained with the LEHR collimator used in the study, *HMR4HSTD* HMR4H values calculated for a standard medium-energy collimator (*see* section Myocardial image acquisition and analysis), *HC* healthy controls, *MSA* multiple system atrophy, *PSP* progressive supranuclear palsy, *PARK2* symptomatic carriers of mutations in the Parkin gene, *PARK8* symptomatic carriers of mutations in the LRRK2 gene, *iPD* idiopathic Parkinson's disease, *iRBD* idiopathic REM sleep behaviour disorder, *PARK1* symptomatic carriers of E46K mutation in the SNCA gene; *DLB* dementia with Lewy bodies. The *continuous red line* indicates the optimal $HMR4H_{LEHR}$ and $HMR4H_{STD}$ cut-off values (1.72 and 2.15, respectively) for discriminating patients with iPD, iRBD, PARK or DLB from HC as determined using the classification and regression tree algorithm and ROC analysis. The *discontinuous red line* indicates the optimal $HMR4H_{LEHR}$ and $HMR4H_{STD}$ cut-off values (1.40 and 1.64, respectively) for discriminating patients with iRBD, PARK, or DLB from HC. Statistically significant ($p < 0.05$) group comparisons using Kruskal-Wallis ANOVA are indicated as follows: $^{*}p < 0.05$, $^{**}p < 0.005$, $^{***}p < 0.001$, vs. HC; $^{\wedge}p < 0.05$, $^{\wedge\wedge}p < 0.005$, $^{\wedge\wedge\wedge}p < 0.001$, vs. MSA; $^{\#}p < 0.05$, vs. PSP; $^{\%}$ for $p < 0.05$, vs. PARK8

$HMR4H_{LEHR}$ cut-off value for additionally discriminating patients with the most aggressive LB spectrum phenotypes (iRBD, PARK1 and DLB) was 1.40 ($HMR4H_{STD}$ 1.64). Conversely, the lowest HMR4H classification accuracies (and lowest improvements from baseline accuracies) were obtained for strategies including only patients with parkinsonisms with mild or absent LB pathology (PARK8, PARK2, PSP and MSA), particularly when HMR4H values in patients with MSA were compared with those in HC. In the CART analysis, for most HMR4H classification strategies including patients with MSA, the optimal cut-off value was undetermined, supporting the presence of marked differences between patients with MSA and other patient groups, and similarities in terms of MIBG uptake between patients with MSA and HC.

Table 1 shows the demographic and clinical characteristics of the study population. All groups were comparable in terms of age and gender, with no statistically significant differences except for the age of DLB patients who were older than PARK1 carriers and HC. The prevalence of diabetes mellitus was comparable between the groups (average 12.5% to 16.7%) except in patients with PSP in whom it was higher but not statistically significant. Disease duration averaged 3.55 to 5.63 years, with no statistically significant differences between groups except in patients with PARK2 and PARK8 in whom disease duration was significantly longer. HMR wash-out was in line with the pattern observed for separated HMR values, with the lowest HMR wash-out percentages in HC and patients with MSA and the highest in patients with iPD, PARK1 and DLB. There were no statistically significant differences in myocardial MIBG metrics between diabetic and nondiabetic patients within each group (data not shown). We also evaluated the correlation between MIBG measures, age and disease duration in patients, and found that age (but not disease duration) was significantly ($p < 0.05$) correlated with HMR15M and HMR4H in all study groups.

Regarding the classification performance of the identified optimal $HMR4H_{LEHR}$ cut-off values, using a $HMR4H_{LEHR}$ cut-off value of 1.40 ($HMR4H_{STD}$ 1.64), in our study population myocardial MIBG uptake would have been classified as abnormal in two HC (4.4%), 5 MSA patients (12.5%), 2 PSP patients (16.7%), 2 PARK2 patients (25.0%), 11 PARK8

Table 1 Demographic data, frequency of diabetes, disease duration and myocardial MIBG uptake ratios for early and delayed anterior scintigraphy images in all diagnostic groups

	HC	MSA	PSP	PARK2	PARK8	iPD	iRBD	PARK1	DLB
No. of subjects	45	40	12	8	22	85	6	4	17
Age (years)	61.84 (11.86)[I]	62.83 (7.96)	68.25 (6.88)	63.35 (8.64)	64.28 (10.26)	65.01 (10.03)	67.02 (4.56)	52.71 (5.93)	70.96 (3.84)[a,h]
Male, *n* (%)	22 (48.90)	18 (45.00)	7 (58.30)	3 (37.50)	12 (54.50)	48 (56.50)	5 (83.30)	2 (50.00)	10 (58.80)
Diabetes, *n* (%)	7 (15.90)	6 (15.00)	4 (33.30)	1 (12.50)	3 (13.60)	13 (15.30)	1 (16.70)	0	0
Disease duration (years)	–	3.93 (3.13)[d,e]	3.55 (2.07)[d]	26.06 (13.61)	8.52 (5.36)	5.63 (5.17)[d]	3.89 (2.95)	3.94 (3.41)	4.86 (2.31)
$HMR15M_{LEHR}$	1.86 (0.20)[e,f,g,h,i]	1.83 (0.39)[f,g,h]	1.68 (0.16)	1.58 (0.30)	1.58 (0.31)	1.50 (0.32)[a,b]	1.31 (0.12)[a,b]	1.30 (0.16)[a]	1.36 (0.18)[a,b]
$HMR4H_{LEHR}$	1.86 (0.26)[e,f,g,h,i]	1.82 (0.37)[f,g,h,i]	1.59 (0.23)[f]	1.51 (0.30)	1.51 (0.32)[a,h]	1.38 (0.29)[a,b]	1.23 (0.09)[a,b]	1.20 (0.09)[a,b]	1.17 (0.11)[a,b,c,e]
$HMR15M_{STD}$	2.37 (0.32)[e,f,g,h,i]	2.34 (0.63)[f,g,i]	2.08 (0.25)	1.93 (0.47)	1.92 (0.49)[a]	1.80 (0.51)[a,b]	1.50 (0.19)[a,b]	1.48 (0.25)[a]	1.57 (0.29)[a,b]
$HMR4H_{STD}$	2.37 (0.42)[e,f,g,h,i]	2.30 (0.58)[f,g,h,i]	1.93 (0.37)[f]	1.81 (0.47)	1.81 (0.50)[a,i]	1.60 (0.46)[a,b]	1.37 (0.14)[a,b]	1.32 (0.14)[a,b]	1.28 (0.18)[a,b,c,e]
HMRW	−1.60 (11.86)[f,i]	−0.11 (15.29)[f]	+6.00 (10.71)	+4.30 (13.12)	+3.87 (10.85)	+7.84 (10.42)[a,b]	+5.51 (8.90)	+7.13 (7.25)	+11.46 (0.99)[a]

The data presented are means (standard deviation), unless otherwise specified

Abbreviations: *HC* healthy controls, *MSA* multiple system atrophy, *PSP* progressive supranuclear palsy, *PARK2* symptomatic carriers of mutations in the Parkin gene, *PARK8* symptomatic carriers of mutations in the LRRK2 gene, *iPD* idiopathic Parkinson's disease, *iRBD* idiopathic REM sleep behaviour disorder, *PARK1* symptomatic carriers of E46K mutation in the SNCA gene, *DLB* dementia with Lewy bodies, *HMR* heart-to-mediastinum ratio, *HMR15M* HMR for MIBG uptake in the early phase (15 min), *HMR4H* HMR for MIBG uptake in the delayed phase (4 h), $HMR15M_{LEHR}$ and $HMR4H_{LEHR}$ calculated HMR15M and HMR4H for the low-energy high-resolution collimator used in the present study, $HMR15M_{STD}$ and $HMR4H_{STD}$ standardized HMR15M and HMR4H values for a standard medium-energy collimators based on LEHR data from the present study, as determined by the formula provided by Verschure et al. [17], *HMRW* HMR washout of MIBG as calculated using the following formula $[(HMR15M_{LEHR} - HMR4H_{LEHR})/HMR15M_{LEHR}] \times 100$

Statistically significant ($p < 0.05$) results in the Kruskall-Wallis ANOVA test for group comparisons: [a] versus HC, [b] versus MSA, [c] versus PSP, [d] versus PARK2, [e] versus PARK8, [f] versus iPD, [g] versus iRBD, [h] versus PARK1, [I] versus DLB

patients (50.0%), 45 iPD patients (52.9%), 6 iRBD patients (100%), 17 DLB patients (93.3%) and 4 PARK1 patients (100%). Using a $HMR4H_{LEHR}$ cut-off value of 1.72 ($HMR4H_{STD}$, 2.15), myocardial MIBG uptake would have been classified as abnormal in 6 HC (13.3%), 15 MSA patients (37.5%), 8 PSP patients (66.7%), 5 PARK2 patients (62.5%), 16 PARK8 patients (72.7%), 72 iPD patients (84.7%), 6 iRBD patients (100%), 17 DLB patients (100%) and 4 PARK1 patients (100%).

Lastly, regarding diagnostic accuracy using HMR15M values, ROC analysis showed a similar pattern to HMR4H in which HMR15M had the highest accuracy when the analysis included only patients with the most severe LB pathology (PARK1, DLB, iRBD and iPD; AUC above 0.91) and the lowest accuracy when the analysis included only patients with mild or absent LB pathology (PARK8, PARK2, PSP and MSA; AUC below 0.66). However, the diagnostic performance of HMR15M in terms of specificity and identification of possible cut-off values in the ROC analysis and CART was much worse than that of HMR4H (see Supplementary Fig. 2 and Supplementary Table for further details).

Discussion

In the present study, we analysed myocardial MIBG scintigraphy patterns in patients with a wide variety of idiopathic and genetic parkinsonisms characterized by different degrees of LB pathology. Our results, supported by the inclusion of patients with genetic PD variants, further validate the usefulness of myocardial MIBG scintigraphy for discriminating LB spectrum disorders (PARK1, DLB, iRBD and iPD) both from HC and from patients with parkinsonisms with milder or absent LB pathology (PARK2, PSP or MSA). We also observed that in our centre a $HMR4H_{LEHR}$ cut-off value of 1.40 ($HMR4H_{STD}$ of 1.64) would correctly identify 93% to 100% of patients with the most aggressive LB diseases (PARK1, DLB and iRBD) and a $HMR4H_{LEHR}$ cut-off value of 1.72 ($HMR4H_{STD}$ of 2.15) would additionally identify up to 85% of iPD patients.

The analysis of patients with various genetic PD variants enabled us to study homogeneous patient groups, including those with genotypes with a high LB burden (PARK1 mutations), those with genetic variants with varying degrees of LB pathology (PARK8) and those with mild or absent LB (PARK2). Previous studies performed by our group have indicated that the analysis of neurovascular dysfunction and myocardial sympathetic denervation may be helpful for discriminating patients with PD genotypes associated with marked LB pathology [10, 12, 22], which is in line with the findings of other studies demonstrating myocardial denervation in patients with idiopathic LB spectrum disorders [3, 6, 23, 24]. The present study also demonstrated that myocardial MIBG imaging is helpful for discriminating MSA patients from iPD patients, as previously found even for early disease stages [4, 25]. In addition, our work illustrates the presence of exceptions in MIBG uptake patterns. For example, while as expected most iPD patients (53% to 85%) had abnormal MIBG imaging and most MSA patients (62% to 87%) had normal MIBG imaging, a considerable number of patients in both groups did not follow this pattern.

Table 2 CART classification accuracies and optimal HMR4H cut-off values for discriminating healthy controls from patients grouped in different classification schemes

Classification scheme	Accuracy (%)			Optimal cut-off values	
	Training	Baseline	Cross-validation	$HMR4H_{LEHR}$	$HMR4H_{STD}$
S1 (DLB + PARK1 + iRBD)	97.22	62.50	97.22	1.40	1.64
S2 (S1 + iPD)	88.67	71.70	87.42	1.73	2.16
S3 (S2 + PARK8 + PARK2)	85.71	76.19	83.07	1.73	2.16
S4 (S3 + PSP)	84.08	77.61	81.09	1.72	2.15
S5 (S4 + MSA)	81.33	81.33	81.33	Not determined	Not determined
S6 (iPD + PARK8 + PARK2 + PSP + MSA)	78.97	78.97	78.04	Not determined	Not determined
S7 (PARK8 + PARK2 + PSP + MSA)	76.38	64.57	62.20	Not determined	Not determined
S8 (PSP + MSA)	63.92	53.61	56.70	1.67	2.07
S9 (MSA)	64.71	52.94	57.65	1.67	2.07

Abbreviations: *HMR4H* delayed (4 h) heart-to-mediastinum MIBG uptake ratio on anterior scintigraphy images, $HMR4H_{LEHR}$ HMR4H values from the original study data obtained with a low-energy high-resolution collimator, $HMR4H_{STD}$ equivalent standardized HMR4H values calculated for a medium-energy collimators, *MSA* multiple system atrophy, *PSP* progressive supranuclear palsy, *PARK2* symptomatic carriers of mutations in the Parkin gene, *PARK8* symptomatic carriers of mutations in the LRRK2 gene,*iPD* idiopathic Parkinson's disease, *iRBD* idiopathic REM sleep behaviour disorder, *PARK1* symptomatic carriers of E46K mutation in the SNCA gene, *DLB* dementia with Lewy bodies

In our study, MIBG measures were not significantly related to disease duration or other influencing factors such as diabetes. Furthermore, we did our best to exclude patients with clinical and imaging data suggestive of structural heart disease. In iPD patients, one of the potential influencing factors for MIBG imaging misclassification may be related to the well-known clinical and pathogenic variability of iPD [26], which might be linked to the variability in LB pathology in iPD and, hence, to the variability in the degree of myocardial denervation. In line with this idea, we believe that myocardial MIBG imaging might be a good tool to identify patients with iPD heavily driven by LB pathology. In the case of MSA patients with abnormal myocardial MIBG imaging, although the reasons for this finding remain unknown, some authors have suggested that it may be due to trans-synaptic degeneration or to a concomitant LB disorder [27]. Other authors have also suggested that MSA patients may develop LBs over the years [28]. LBs have been observed in sympathetic ganglia in some MSA patients, potentially favouring lower myocardial MIBG uptake [29].

We found that HMR4H had outstanding accuracy in discriminating patients with LB disorders from HC. Moreover, we found that in our centre a $HMR4H_{LEHR}$ cut-off value of 1.40 ($HMR4H_{STD}$ of 1.64) was optimal for discriminating HC from patients with the most aggressive LB disorders (DLB, PARK1 and iRBD) and that a $HMR4H_{LEHR}$ cut-off value of 1.72 ($HMR4H_{STD}$ of 2.15) was also optimal for discriminating most iPD patients. Our findings are comparable to the results of a comprehensive meta-analysis of 46 myocardial ^{123}I-MIBG studies that used similar imaging equipment (triple-headed or double-headed gamma camera with LEHR collimators) and included a total of 2,680 participants with various neuropsychiatric and movement disorders [30]. The authors concluded that the best $HMR4H_{LEHR}$ threshold for discriminating a cluster of patients with LB disorders (PD, DLB and iRBD) from another cluster of patients with CNS neurodegenerative conditions harboring low or absent LB pathology (Alzheimer's disease, MSA, PSP, vascular dementia and frontotemporal dementia) was 1.77, which is close to the optimal $HMR4H_{LEHR}$ cut-off value of 1.72 that we found for differentiating HC (absent LB pathology) from patients with LB disorders (iPD, iRBD, DLB and PARK1). Regarding the optimal $HMR4H_{LEHR}$ cut-off value of 1.40 for discriminating patients with severe LB disorders (iRBD, DLB and PARK1) from HC, although the meta-analysis did not provide specific $HMR4H_{LEHR}$ thresholds to discern patients with most severe LB disease phenotypes, it is noteworthy that in most individual studies of the meta-analysis including patients with DLB and iRBD, the average $HMR4H_{LEHR}$ values were below 1.40.

One of the strongest methodological advantages of our study was that we excluded and controlled for confounding factors in myocardial MIBG imaging including drugs, diabetes and structural myocardial abnormalities. Overall, the prevalence of diabetes in our study population ranged from 12.5% to 16.7% in both patients and HC. In our study the presence of diabetes did not significantly influence differences in scintigraphy metrics. It has been postulated that a delayed MIBG HMR cut-off lower than 1.7 is a predictor of a poor prognosis for heart disease development [31]. To reduce the possibility of including patients with significant structural heart disease or heart failure, we first performed a

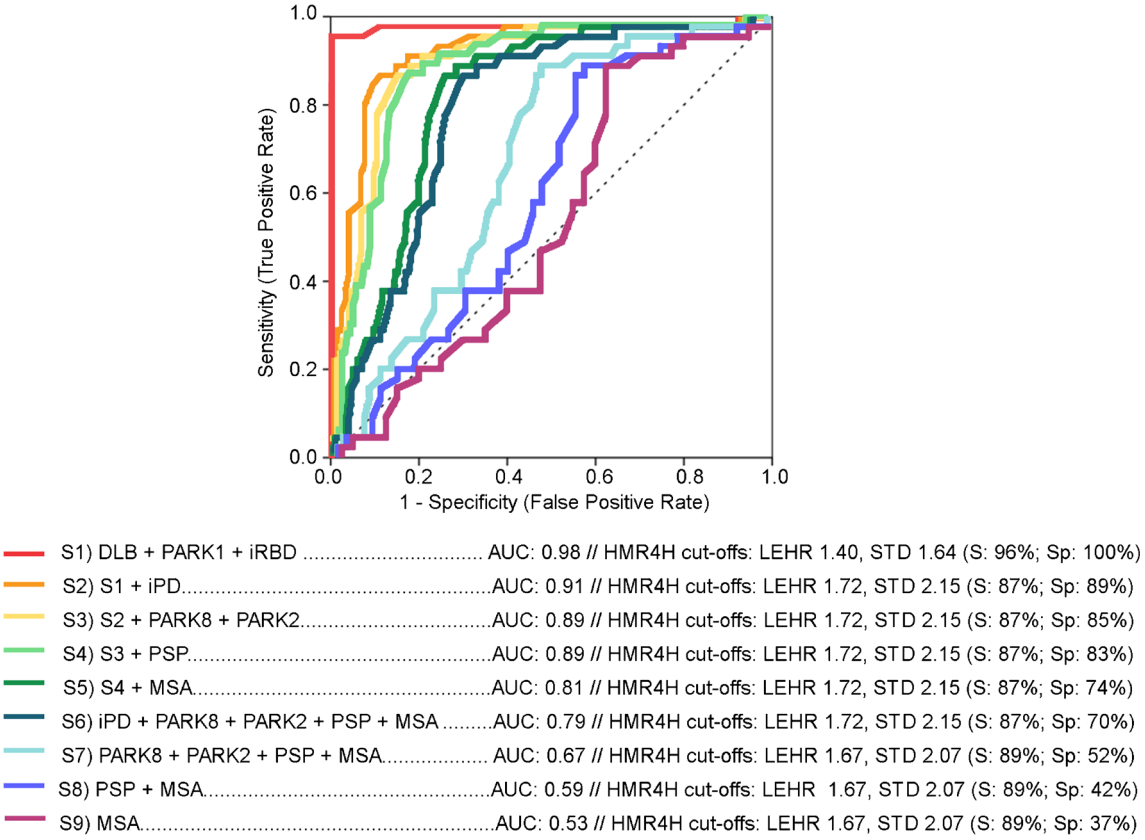

Fig. 2 Nonparametric receiver operating characteristic (ROC) analysis and respective optimal HMR4H cut-off values for discriminating healthy controls from patients grouped according to different classification schemes, with one ROC curve for each classification scheme. The AUC and optimal HMR4H cut-off value with its respective sensitivity and specificity are also shown for each ROC curve. Abbreviations: *AUC* area under the curve, *HMR4H* late (4 h) heart-to-mediastinum MIBG uptake on anterior scintigraphy images, *LEHR* HMR4H values for the low-energy high-resolution collimator used in the study, *STD* HMR4H values calculated for a standard medium-energy collimator, *S* sensitivity (%), *Sp* specificity (%), *MSA* multiple system atrophy, *PSP* progressive supranuclear palsy, *PARK2* symptomatic carriers of mutations in the Parkin gene, *PARK8* symptomatic carriers of mutations in the LRRK2 gene, *iPD* idiopathic Parkinson's disease, *iRBD* idiopathic REM sleep behaviour disorder, *PARK1* symptomatic carriers of E46K mutation in the SNCA gene, *DLB* dementia with Lewy bodies

comprehensive review of electronic clinical records. In addition, we obtained ECG-gated ^{99m}Tc-6-MIBI SPECT images under resting conditions to identify and quantify abnormalities in global and regional myocardial perfusion, left ventricular ejection fraction, total diastolic and systolic volumes and ventricular wall movement abnormalities. All patients with any MIBI SPECT abnormalities suggestive of structural heart disease or heart failure were subsequently evaluated by a cardiologist who discarded the presence of any heart conditions by clinical interview, physical examination and appropriate ancillary evaluations (electrocardiography and echocardiography, among others).

There were some limitations in this study that should be mentioned. First, because the study was a retrospective analysis of historical clinical data, we were not able to obtain consistent measurements of the PD motor status from participants such as Unified Parkinson's Disease Rating Scale (UPDRS) or Hoehn and Yahr scores. These clinical measures would have been extremely useful to understand the association between different motor profiles and the degree of myocardial denervation on MIBG scintigraphy. Second, the generalizability of the proposed optimal HMR4H cut-off values ($HMR4H_{LEHR}$ 1.40 and 1.72, $HMR4H_{STD}$ 1.64 and 2.15) from one imaging centre to another might be difficult, since HMR values are highly dependent on the characteristics of the collimator, on the software used and on the placement of the heart and mediastinum ROIs. To overcome the variability related to the characteristics of the collimator, in addition to providing the raw HMR values obtained using our LEHR collimator, we also included standardized HMR values adapted to the more widely used and recommended ME collimators [16]. However, these HMR cut-off values should be used with caution, as other biases may have been introduced in relation to variability in MIBG image acquisition and analysis methods. Third, although we reasonably excluded patients with structural heart disease or heart failure, we could not completely rule out the presence of microvascular dysfunction of the heart in all patients, an abnormality potentially inducing impairment in myocardial sympathetic activity (MIBG uptake) and causing subtle heart

failure with normal ejection fraction. Lastly, the numbers of patients in some of the diagnostic groups (particularly PARK1, PARK2 and iRBD) were small, a limitation that may have influenced the statistical power of the analysis and the generalizability of the results. To overcome this limitation, we used nonparametric statistical analyses and also step-wise grouping of patients when comparing groups and for obtaining diagnostic MIBG uptake cut-off values. It is also important to consider that genetic PD variants are rare and identification of such patients is uncommon in clinical routine. This is especially true for SNCA-linked mutations (PARK1), which are considered a rare condition as they are limited to specific families and series around the world.

In conclusion, based on the analysis of patients with a wide range of idiopathic and genetic variants of PD known to have different degrees of LB pathology, our study supports the validity of myocardial MIBG scintigraphy as a biomarker to identify patients with LB spectrum disorders. The finding that symptomatic carriers of PARK1 mutation have delayed HMRs comparable to those of patients with DLB and iRBD, both being diseases characterized by the presence of LBs, supports this hypothesis.

Authors' contributions I.G., V.L. and J.C.G.-E. designed the study, and I.G., V.L., T.R., J.C.G.-E., A.M.-G. and BT collected the data. I.G., V.L. and J.C.G.-E. supervised the study. I.G., J.C. and J.C.G.-E. did the statistical analysis, and I.G. and V.L. created the figures and tables. I.G., V.L. and J.C.G.-E. interpreted the results of the analysis with subsequent substantial contributions from all the coauthors. I.G., V.L. and J.C.G.-E. drafted the manuscript, to which all the authors contributed with revisions, and all the authors approved the final version.

Funding This study was funded by Michael J. Fox Foundation via the RRIA (Rapid Response Innovation Awards) 2014 Program (grant ID 10189) and the Instituto de Salud Carlos III through the project PI14/00679 and Juan Rodes grant JR15/00008 (I.G.; cofunded by the European Regional Development Fund/European Social Fund 'Investing in Your Future').

Compliance with ethical standards

Conflicts of interest None.

Ethical approval All procedures performed in studies involving human participants were in accordance with the ethical standards of the institutional and/or national research committee and with the principles of the 1964 Declaration of Helsinki and its later amendments or comparable ethical standards.

Informed consent Informed consent was obtained from all individual participants included in the study.

References

1. Goldstein DS. Sympathetic neuroimaging. Handb Clin Neurol. 2013;117:365–70. https://doi.org/10.1016/B978-0-444-53491-0.00029-8.
2. Orimo S, Ozawa E, Nakade S, Sugimoto T, Mizusawa H. (123)I-metaiodobenzylguanidine myocardial scintigraphy in Parkinson's disease. J Neurol Neurosurg Psychiatry. 1999;67:189–94.
3. Miyamoto T, Miyamoto M, Inoue Y, Usui Y, Suzuki K, Hirata K. Reduced cardiac 123I-MIBG scintigraphy in idiopathic REM sleep behavior disorder. Neurology. 2006;67:2236–8. https://doi.org/10.1212/01.wnl.0000249313.25627.2e.
4. Berganzo K, Tijero B, Somme JH, Llorens V, Sanchez-Manso JC, Low D, et al. SCOPA-AUT scale in different parkinsonisms and its correlation with (123)I-MIBG cardiac scintigraphy. Parkinsonism Relat Disord. 2012;18:45–8. https://doi.org/10.1016/j.parkreldis.2011.08.018.
5. Taki J, Yoshita M, Yamada M, Tonami N. Significance of 123I-MIBG scintigraphy as a pathophysiological indicator in the assessment of Parkinson's disease and related disorders: it can be a specific marker for Lewy body disease. Ann Nucl Med. 2004;18:453–61.
6. Suzuki M, Kurita A, Hashimoto M, Fukumitsu N, Abo M, Ito Y, et al. Impaired myocardial 123I-metaiodobenzylguanidine uptake in Lewy body disease: comparison between dementia with Lewy bodies and Parkinson's disease. J Neurol Sci. 2006;240:15–9. https://doi.org/10.1016/j.jns.2005.08.011.
7. Kashihara K, Imamura T, Shinya T. Cardiac 123I-MIBG uptake is reduced more markedly in patients with REM sleep behavior disorder than in those with early stage Parkinson's disease. Parkinsonism Relat Disord. 2010;16:252–5. https://doi.org/10.1016/j.parkreldis.2009.12.010.
8. Oda H, Ishii K, Terashima A, Shimada K, Yamane Y, Kawasaki R, et al. Myocardial scintigraphy may predict the conversion to probable dementia with Lewy bodies. Neurology. 2013;81:1741–5. https://doi.org/10.1212/01.wnl.0000435553.67953.81.
9. Zarranz JJ, Alegre J, Gomez-Esteban JC, Lezcano E, Ros R, Ampuero I, et al. The new mutation, E46K, of alpha-synuclein causes Parkinson and Lewy body dementia. Ann Neurol. 2004;55:164–73. https://doi.org/10.1002/ana.10795.
10. Tijero B, Gomez-Esteban JC, Lezcano E, Fernandez-Gonzalez C, Somme J, Llorens V, et al. Cardiac sympathetic denervation in symptomatic and asymptomatic carriers of the E46K mutation in the alpha synuclein gene. Parkinsonism Relat Disord. 2013;19:95–100. https://doi.org/10.1016/j.parkreldis.2012.08.001.
11. Singleton A, Gwinn-Hardy K, Sharabi Y, Li ST, Holmes C, Dendi R, et al. Association between cardiac denervation and parkinsonism caused by alpha-synuclein gene triplication. Brain. 2004;127:768–72. https://doi.org/10.1093/brain/awh081.
12. Tijero B, Gabilondo I, Lezcano E, Teran-Villagra N, Llorens V, Ruiz-Martinez J, et al. Autonomic involvement in parkinsonian carriers of PARK2 gene mutations. Parkinsonism Relat Disord. 2015;21:717–22. https://doi.org/10.1016/j.parkreldis.2015.04.012.
13. Valldeoriola F, Gaig C, Muxi A, Navales I, Paredes P, Lomena F, et al. 123I-MIBG cardiac uptake and smell identification in parkinsonian patients with LRRK2 mutations. J Neurol. 2011;258:1126–32. https://doi.org/10.1007/s00415-010-5896-6.
14. Nonnekes J, Timmer MH, de Vries NM, Rascol O, Helmich RC, Bloem BR. Unmasking levodopa resistance in Parkinson's disease. Mov Disord. 2016;31:1602–9. https://doi.org/10.1002/mds.26712.
15. Stefanelli A, Treglia G, Bruno I, Rufini V, Giordano A. Pharmacological interference with 123I-metaiodobenzylguanidine: a limitation to developing cardiac innervation imaging in clinical practice? Eur Rev Med Pharmacol Sci. 2013;17:1326–33.
16. Flotats A, Carrio I, Agostini D, Le Guludec D, Marcassa C, Schafers M, et al. Proposal for standardization of 123I-metaiodobenzylguanidine (MIBG) cardiac sympathetic imaging by the EANM Cardiovascular Committee and the European Council of Nuclear Cardiology. Eur J Nucl Med Mol Imaging. 2010;37:1802–12. https://doi.org/10.1007/s00259-010-1491-4.

17. Verschure DO, Poel E, Nakajima K, Okuda K, van Eck-Smit BL, Somsen GA, et al. A European myocardial (123)I-mIBG cross-calibration phantom study. J Nucl Cardiol. 2018;25:1191–7. https://doi.org/10.1007/s12350-017-0782-6.
18. Inoue Y, Suzuki A, Shirouzu I, Machida T, Yoshizawa Y, Akita F, et al. Effect of collimator choice on quantitative assessment of cardiac iodine 123 MIBG uptake. J Nucl Cardiol. 2003;10:623–32.
19. Perkins NJ, Schisterman EF. The inconsistency of "optimal" cutpoints obtained using two criteria based on the receiver operating characteristic curve. Am J Epidemiol. 2006;163:670–5. https://doi.org/10.1093/aje/kwj063.
20. Hall M, Frank E, Holmes G, Pfahringer B, Reutemann P, Witten IH. The WEKA data mining software: an update. J SIGKDD Explor Newsl. 2009;11:10–8. https://doi.org/10.1145/1656274.1656278.
21. Schisterman EF, Perkins NJ, Liu A, Bondell H. Optimal cut-point and its corresponding Youden index to discriminate individuals using pooled blood samples. Epidemiology. 2005;16:73–81.
22. Tijero B, Gomez Esteban JC, Somme J, Llorens V, Lezcano E, Martinez A, et al. Autonomic dysfunction in parkinsonian LRRK2 mutation carriers. Parkinsonism Relat Disord. 2013;19:906–9. https://doi.org/10.1016/j.parkreldis.2013.05.008.
23. Lamotte G, Morello R, Lebasnier A, Agostini D, Defer GL. Accuracy and cutoff values of delayed heart to mediastinum ratio with (123)I-metaiodobenzylguanidine cardiac scintigraphy for Lewy body disease diagnoses. BMC Neurol. 2015;15:83. https://doi.org/10.1186/s12883-015-0338-9.
24. Miyamoto T, Miyamoto M, Suzuki K, Nishibayashi M, Iwanami M, Hirata K. 123I-MIBG cardiac scintigraphy provides clues to the underlying neurodegenerative disorder in idiopathic REM sleep behavior disorder. Sleep. 2008;31:717–23.
25. Braune S, Reinhardt M, Schnitzer R, Riedel A, Lucking CH. Cardiac uptake of [123I]MIBG separates Parkinson's disease from multiple system atrophy. Neurology. 1999;53:1020–5.
26. Berg D, Postuma RB, Bloem B, Chan P, Dubois B, Gasser T, et al. Time to redefine PD? Introductory statement of the MDS Task Force on the definition of Parkinson's disease. Mov Disord. 2014;29:454–62. https://doi.org/10.1002/mds.25844.
27. Nagayama H, Ueda M, Yamazaki M, Nishiyama Y, Hamamoto M, Katayama Y. Abnormal cardiac [(123)I]-meta-iodobenzylguanidine uptake in multiple system atrophy. Mov Disord. 2010;25:1744–7. https://doi.org/10.1002/mds.23338.
28. Sone M, Yoshida M, Hashizume Y, Hishikawa N, Sobue G. α-Synuclein-immunoreactive structure formation is enhanced in sympathetic ganglia of patients with multiple system atrophy. Acta Neuropathol. 2005;110:19–26. https://doi.org/10.1007/s00401-005-1013-9.
29. Orimo S, Kanazawa T, Nakamura A, Uchihara T, Mori F, Kakita A, et al. Degeneration of cardiac sympathetic nerve can occur in multiple system atrophy. Acta Neuropathol. 2007;113:81–6. https://doi.org/10.1007/s00401-006-0160-y.
30. King AE, Mintz J, Royall DR. Meta-analysis of 123I-MIBG cardiac scintigraphy for the diagnosis of Lewy body-related disorders. Mov Disord. 2011;26:1218–24. https://doi.org/10.1002/mds.23659.
31. Nagamachi S, Fujita S, Nishii R, Futami S, Tamura S, Mizuta M, et al. Prognostic value of cardiac I-123 metaiodobenzylguanidine imaging in patients with non-insulin-dependent diabetes mellitus. J Nucl Cardiol. 2006;13:34–42. https://doi.org/10.1016/j.nuclcard.2005.11.009.